Seasonal Evaluation of Storm Life Cycles in the CONUS from 12 Years of Radar-Based Storm Tracks

AODHAN SWEENEY*

National Weather Center Research Experiences for Undergraduates Program
Norman, Oklahoma

CAMERON HOMEYER, AMY MCGOVERN, RYAN LAGERQUIST AND THEA SANDMÆL
University of Oklahoma
Norman, Oklahoma

ABSTRACT

While there is considerable knowledge of the global distribution of precipitation, lightning, and severe weather, little is known about the statistics of storm life cycles responsible for these phenomena. Previous studies have used long-term and large-scale data related to severe storms, but never for a survey on the trends of these storms over the CONUS. An objective, long-term study that looks into basic characteristics such as duration, path, speed, or the geographic/diurnal/seasonal variability of storms would shed light on their fundamental trends over the CONUS. A question that may arise is "why has this type of survey not yet been done?". This is due to two reasons: 1) lack of a suitable storm tracking algorithm capable of identifying and stitching storms for this type of project, and 2) no single dataset with complete radar composites over a sufficiently long period. With a specific tracking algorithm generated for this project and the availability of storm track data in the MYRORSS (Multi-Year Reanalysis of Remotely Sensed Storms) database, a primary survey was conducted. Storm activity was found to reach its maximum over the Southeastern United States and showed signatures of orographic forcing in the west. Statistical trends showed consistency across seasons in average lifetime and direction of storms, but variation among average speed and spatial expanse.

1. Introduction

To investigate storms and their spatial/temporal characteristics, the first step is identifying and tracking these objects from radar. This requires a storm tracking algorithm, and more specifically one that looks at radar reflectivity to find convective signatures. Preliminary storm tracking algorithms focused on single satellite image thresholds to identify storms Augustine and Howard (1988). A global threshold like this one is subject to the main problem that it cannot distinguish between noisy points that fluctuate above the given threshold and new spawning cells with only a few data points of sufficient intensity. Other previous methods have used a combination of thresholds and a hysteresis technique where false cells are prohibited from spawning by a lagging technique to double check noisy data (Jain 1989). In the context of image processing, the hysteresis technique utilizes two thresholds: a lower one to initially start the storm identification and a higher one that requires a certain amount of contiguous pixels for that storm identification to continue. This method is able to differentiate from random noise because although certain pixels may be above the secondary given threshold, they will either a.) not be contiguous or b.) not have a sufficient amount of surrounding pixels above the primary threshold. Although these methods are effective, they lead to a heavy reliance on heuristics and cannot be generalized to all types of geospatial imaging.

Later methods of tracking algorithms identified storms using a watershed transform technique of region-based object identification (Lakshmanan et al. 2009). This technique works by "flooding" the image from top to bottom (global max to global min) in a process called immersion whereby values are sifted through pixel by pixel identifying the lowest adjacent value and following that pixel down until a local minimum is found as well as its surrounding area called a basin. In the case of storm identification, this idea is flipped and the image is flooded from bottom up, following pixels with highest values of interest so that local maximums may be found and storm ids can be applied. This technique is superior to just use a single or double threshold technique because all local maximums or minimums can be identified in one image sweep (Lakshmanan et al. 2009). In addition, these types of techniques can be used in all types of geospatial imaging.

*Corresponding author address: Aodhan Sweeney Florida State University, 600 West College Ave, Tallahassee Florida)
E-mail: ajs15e@my.fsu.edu

Methods of application of the storm tracking algorithm are either considered casual or non-causal. The casual method uses a real-time application of the storm tracking algorithm, while the non-casual approach waits until all the data is collected. The non-casual approach is an improvement on the former because this allows for any one data point in the track to know the position of future data points and their duration (Lakshmanan et al. 2015). This ability to look backward and forward in time allows for better storm identifications and more coherent tracks. The use of 40-dBZ echo-tops is chosen as a criterion for storm presence in the proposal due to its consistency as a convective signature (Starzec et al. 2017). With a storm tracking algorithm that relies on echo-top altitude from remotely sensed data Homeyer et al. (2017), an objective, long-term, large-scale study is able to be proposed.

Next, a large dataset to apply the tracking algorithm to is needed. Previously, radar algorithms were written to work with single radar data, but better conclusions could be made if nearby radar's data were combined. Merging this radar data helps with radar geometry problems, overlook of geographic features, and better vertical resolution (Lakshmanan et al. 2006). By using intelligent agent formulation, it is possible to take the base radar data and derived products from multiple radars, combine them, and create a single 3D merged grid (Lakshmanan et al. 2006). The culmination of this work resulted in high quality, high-resolution common reference dataset for severe weather referred to as The Multi-Year Reanalysis of Remotely Sensed Storms Project (MYRORSS) (Ortega et al. 2012).

MYRORSS is created with data from the Weather Surveillance Radar 1988 Doppler (WSR-88D) processed by the Warning Decision Support System WDSS (WDSS) and paired with the Multi-Radar Multi-Sensor (MRMS) grids to produce a high-resolution reflectivity dataset (Ortega et al. 2012). MYRORSS is compiled into a 0.01° latitude and longitude grid spanning the CONUS from the years of 1998-2011. Current tracks generated from the tracking algorithm span 2000-2011 making a dataset of 12 years.

An objective quantifying study of storm life cycles over the CONUS is a preliminary step in understanding more about storm phenomena in general. For example, knowledge of their duration, path, speed, or geographic/diurnal/annual variability could be used to improve 1) the evaluation of forecast models and mitigation of risk, and 2) the understanding of their linkages to large-scale climate variability. This project leverages 12 years of 5-minute radar-based storm tracks to evaluate the spatial and temporal characteristics of storm life cycles over the contiguous United States. Specific goals are to develop an understanding of the diurnal and annual cycles and the geographic distribution of storm path characteristics (e.g., duration, path length, speed).

2. Methods

a. Development of Storm Tracking Algorithm

In creating a storm tracking algorithm, baseline approaches to storm tracking algorithms described in the introduction have often been successful but frequently overestimate or underestimate the number of storms created. In this paper, a version of the echo-top tracking algorithm described in Homeyer et al. (2017) is used. Storms are identified by finding a local maximum in echo-top reflectivity. Contours are then drawn around these local maximum and taken as estimates for the locations of updraft within deep convection.

This method provides continuous storm tracks using a three-step procedure: 1) identify local maxima of the 40-dBZ echo-top that exceed an altitude of 4 km above sea level, 2) link these maxima in consecutive radar volumes if within 15 km of each other within 10 minutes, and 3) retain tracks that persist for at least 15 minutes.

An important characteristic about the storm tracking algorithm is its "look back" technique. This means that the algorithm uses data that has already been compiled (non-casual) and is thus able to know what will happen in future data points. This allows the tracking algorithm to make better judgments on storm tracks and cell genesis.

The characteristics of the track created are also separated into three categories: birth, death, and passage. Birth refers to the characteristics of the storm associated with its first occurrence in the dataset, like time and position. Death refers to the characteristics of the storm in its last occurrence in the dataset. Passage refers to all data points collected between the birth and death of the storm object. Defining these differences allows for a more thorough investigation of the characteristics of storm development and evolution over the CONUS.

b. Methods Employed in 12 Year CONUS Review

For the purposes of identifying storm characteristics, the definition of storms is changed slightly from those of (Homeyer et al. 2017). Storm tracks span a 12-year period from the beginning of 2001 to the end of 2011 in 5-minute increments. In this paper, storms are defined as 40-dBZ echo-tops, that persist for a minimum of 15 minutes, at a height greater than 4 km above sea level. The results are evaluated temporally to examine diurnal and seasonal cycles, and spatially investigate where storms are most active. Spatial data is mapped to an equal area grid spanning from -130°E to -60°E in longitude and 20°N to 55°N latitude with 10×10 km resolution. Storms are then binned based on birth, death, and passage to stress where the objects begin, where they end, and where they travel during their lifetimes. Other areas of interest include questions focusing on lifetime, maximum spatial expanse, distance traveled, velocity, and speed of storms over the CONUS.

3. Data

Data used in the analysis is taken from the MYRORSS dataset. Tracks are re-processed to only include 40-dBZ echo-tops that are at a minimum altitude of 4km above sea level. Objects are only counted as real storm cells if they last more than 15 minutes (900 seconds). The data is then binned in various ways looking for possible trends in the set. Temporal characteristics of the data are examined through both a seasonal and diurnal lenses. Spatial properties of these storms are looked at to find where storms happen over the CONUS. Additionally, these primary investigations brought other areas of interest into focus. Seasonal filters, defining winter as Dec-Feb, spring as Mar-May, summer as Jun-Jul, and fall as Sep-Nov.

Data coming from the MYRORSS dataset is fed by the NEXRAD network and thus updates with 5-minute intervals. Because of this, storm objects are seen as snapshots throughout their lives as opposed to temporally seamless tracks. After the data is pooled together, the storm tracking algorithm is applied to the dataset and various types of information are extracted from each observation. This data is then saved for further analysis. The types of data gathered from these observations are contained in the sample data table provided (Table 1). Storms that have been linked together share a common storm identification and can be found in the storm ID column (Table 1).

From this data, the temporal and spatial characteristics of these storms are examined. In both types of characteristics, birth, death, and passage are investigated. Storms are binned in 24 one-hour time steps to find what hours of the day have the highest rates of storm activity. Storm birth is defined as the first instance that the storm tracking algorithm has identified a storm object. Similarly, identifying the last time a unique storm id shows up in the dataset will correspond to the hours with the highest rates of death. It should be noted that because of the 5-minute incremental data between radar imaging, these times for birth and death could have occurred within the gaps of data and are subject to about ± 5 minutes. The passage of these storms includes all the hours that any storm may pass through. Times are rounded to the nearest hour for binning. A final temporal characteristic that was looked into is the lifetime of a storm. This refers to the amount of time passed between the first identification of a storm and the time of its death.

Regarding the spatial characteristics of the storms, a similar evaluation was made for the birth, death, and passage of each storm. The key difference is that now instead of the time associated with each identification, the latitude and longitude of the id taken from the MYRORSS dataset is saved, and plotted on an equal area 10×10 km resolution mapping of the CONUS. Like before, spatial birth refers to the first location of the unique storm ID, and death refers to its last. Passage will correlate to all grid cells that the individual storm IDs passes through.

Additional characteristics examined were the size of the storm, and the distance traveled by the storm. The size of the storm is found by taking the area in km^2 of the polygon created by the storm tracking algorithm around the 40-dBZ echo-top signature. Because there are multiple readings for many storms, any storm that persists more than 10 minutes will have multiple polygons assigned to it throughout its life. In this operational definition of storm size, only the largest area polygon of any storm is examined based on the season.

For distance traveled the arc length of the great circle passing through the first and last position of the storm identification is used. This method is different from finding the full path of the storm because most storms do not travel in a straight line. It should be noted that the point of initiation is the first point where the storm was initially created, not the point after it has existed for 15 minutes.

Finally, the velocity dispersions and speeds of storms were also examined. The velocities of the storms were found for storms that lasted longer than 15 minutes, but once that object was identified as a storm, all velocities in its lifetime were examined. To find seasonal velocity dispersions, a storm's directional velocity is averaged throughout its lifetime. These are then compiled into seasonal graphs. In a similar fashion, speeds are found at each point in a storm's lifetime and averaged. Again, data is separated by season.

4. Analysis

Analysis of the storm life cycles over 12 years will be divided into sections that resemble those of the data section. Primarily, temporal characteristics of the storms will be discussed, followed by spatial characteristics, and finally answers to questions developed along the way. All statistics of any question asked are placed in (Table 1) and (Table 2).

a. Temporal

When looking at birth, death, and passage of storms it is found that summer months show the vast majority of storm activity. The next most active season in storm activity is fall, followed by spring and then winter. The curves for birth, passage, and death are plotted in (Fig. 1), (Fig. 2), (Fig. 3) respectively. All three curves show very similar shapes with their peak occurring during hour 22 UTC time and the hours of most activity being between hours 19 and 24 UTC. One observation to note is the similarity between storm birth and death. Because the diurnal trends appear to be the same, one can draw the logical conclusion that most storms do not last over an hour.

TABLE 1. Sample storm object table. This is what a post processed data from MYRORSS looks like after the storm tracking algorithm has been applied. The table is representative of an early storm on April 1st 2011.

$storm-id$	$unix-time$	$east-velocity$	$north-velocity$	$latitude$	$longitude$	age
00007120110401	1301659212	5.0	10.0	27.55	283.02	0

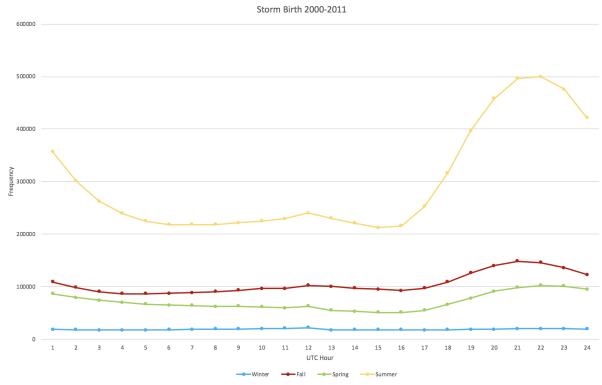

FIG. 1. Line plot showing the differences in storm birth between season. Plotted over one diurnal cycle to show times in UTC of largest storm birth activity. Peak occurs between hours of 19 and 24 UTC.

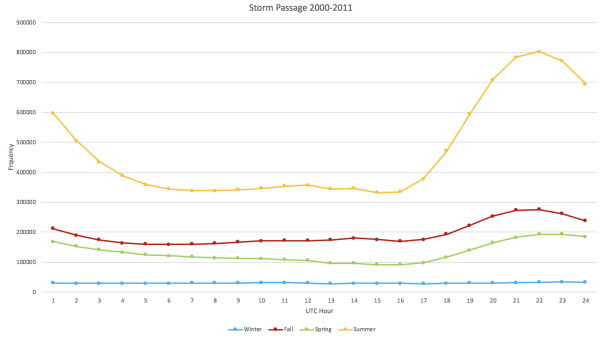

FIG. 2. Line plot showing the differences in storm passage between season. Plotted over one diurnal cycle to show times in UTC of largest storm birth activity. Peak occurs between hours of 19 and 24 UTC.

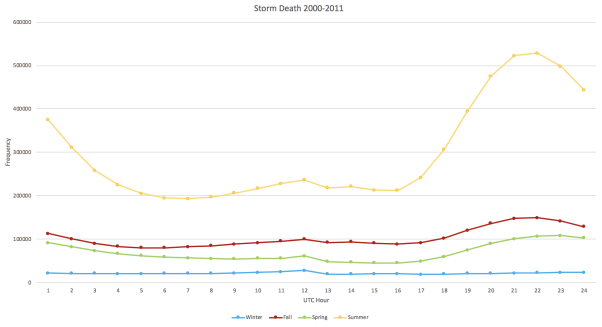

FIG. 3. Line plot showing the differences in storm death between season. Plotted over one diurnal cycle to show times in UTC of largest storm birth activity. Peak occurs between hours of 19 and 24 UTC.

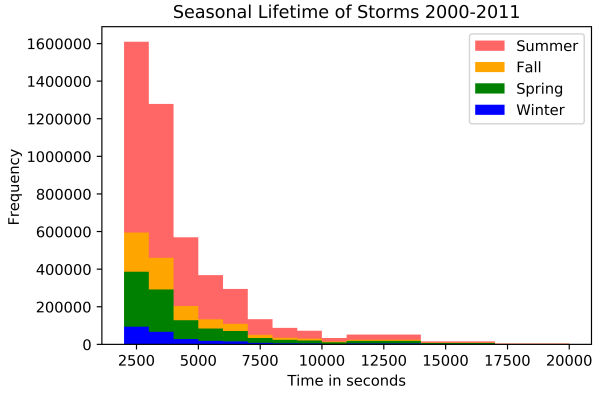

FIG. 4. Histogram showing the differences in storms lifetime with respect to season.

Following this idea, the average length of time that a 40-dBZ echo-top persists based on the season was also examined. Consistent with the diurnal cycles for storm birth and death, most storms did not last more than one hour. It is also found that there is very little variation in storm lifetime across seasons. The shortest lifetime occurs in winter with 44 min, and the longest occurs in summer with a mean lifetime of 46.5 min (Fig. 4).

b. Spatial

Spatial characteristics of birth death and passage focused on the location over the CONUS where the respective event occurred. In all filters created, the Southeastern CONUS is the most active location for storm activity. Again, it is seen that winter is the least active of the seasons and that summer is most active. In addition to the Southeast, Arizona, and New Mexico are also very active regions of storm activity. Perhaps the most interesting of the maps is that of spatial passage in the summer. Large numbers of storms pass over the Gulf seaboard, Florida, the Gulf Stream off the coast of North Carolina, and signatures of orographic forcing in the Western CONUS. Maps of CONUS with highlighted regions of storm birth, passage and death are shown in (Fig. 5), (Fig. 6), and (Fig. 7) respectively.

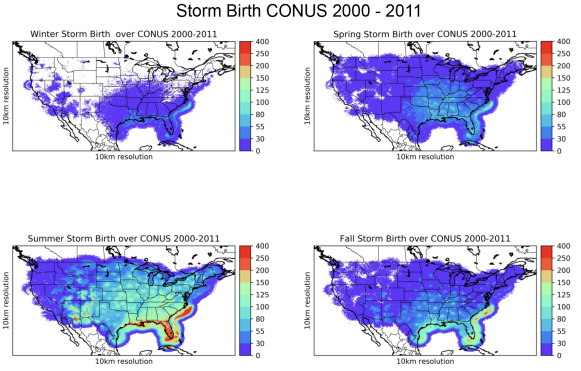

FIG. 5. Map depicting where in CONUS storms are most frequently born split by season.

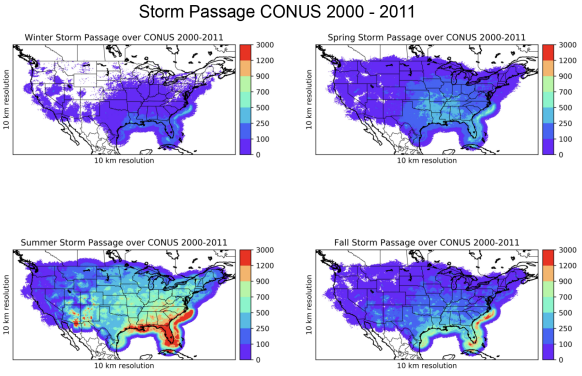

FIG. 6. Map depicting where in CONUS storms most frequently pass over split by season.

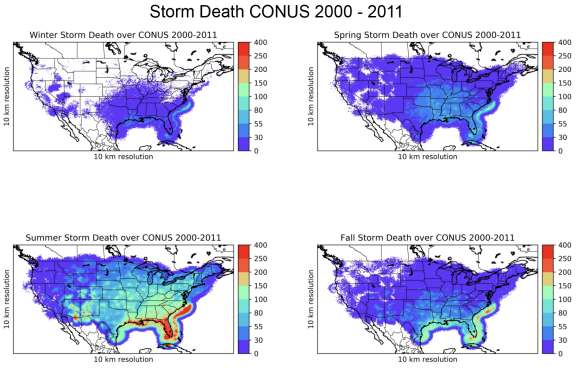

FIG. 7. Map depicting where storms in CONUS storms most frequently die split by season.

One unexpected feature about the spatial mappings is a bias of storm detection local to the radar. This feature appears in concentric rings surrounding NEXRAD radars. The presence of this bias is assumed to be because of the criteria included in the tracking algorithm, and over-registering local radar signatures. It is likely that the cause of this bias is non-meteorological radar return or low-level precipitation in the stratiform region. The problem arises through radar limitations. The further the beam travels from its source, the higher the vertical level of the return signature, which could lead to undetected low-level signatures far from the radar. In addition, most 40-dBZ echo-tops are stratiform in nature, and thus near the radar, there is an apparent oversampling of stratiform signatures. In total, this oversampling near the radars is the result of limited vertical sampling rather than relevant convective cores. A discussion of possible solutions to this problem is in the conclusion section.

In addition, the fact that rings are present as opposed to local maxima with linear decent around radar positions is unexpected. This is likely due to the tilts of the radars in NEXRAD. A primary ring directly outside of the cone of silence corresponds to the largest angle and concentric rings with increasing radii occurring outward correspond to tilts with lower angles.

c. Discussion

In light of the results, the first extra question asked was how large 40-dBZ echo-tops were reaching in spatial expanse. Note that, this shows the largest spatial expanse of a 40-dBZ echo-top generated by the tracking algorithm and is not indicative of the storm sizes throughout the storms lifetime. In addition, large linear systems are counted as storms via individual updrafts as indicated by the echo-top. Due to this, we do not see full sized MCSs in the data.

It is found that the largest maximum storm sizes reached occur in summer with a median of 27.55 km^2, and the smallest storms in winter with a median of 15.99 km^2 (Fig. 8). The graphs for all seasons resemble a hyperbolic function. A large number of 40-dBZ echo-tops that have genesis and extinction without ever reaching any sizable area are seen. Because of this, the medians are supplied as opposed to means, and all statistics on both the mean and median can be found in (Table 2) and (Table 3).

Figures depicting the total distance traveled show that during winter storms travel the furthest with a median of 23.3 km and least during summer with a median of 16.06 km (Fig. 9). Spring and fall show similar distances traveled and the shape of their seasonal curves matches well. Additionally, these histograms plotted for the distance traveled show results for the shortest possible distance between the point of creation and termination of the storm, meaning that these results are lower limits. It is noted that the difference in storm distance traveled, and the consistency between storm lifetimes points to a difference in the average speed of a storm with respect to season.

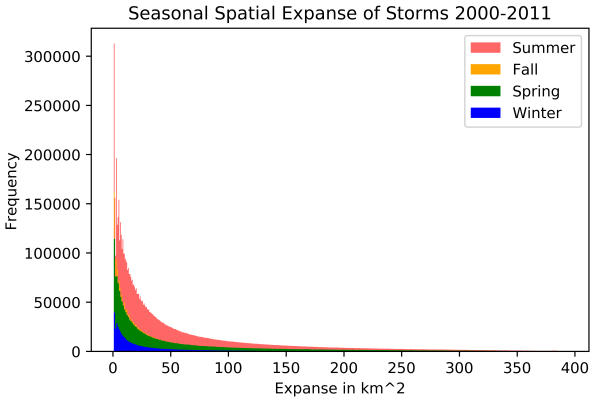

FIG. 8. Histogram of spatial expanse in km^2 based on season. Summertime has largest storms, winter has smallest.

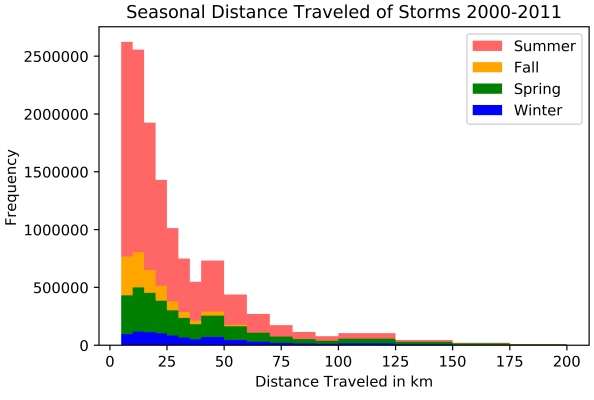

FIG. 9. Histogram showing the distance traveled split up by season. Winter, surprisingly sees furthest traveling storms.

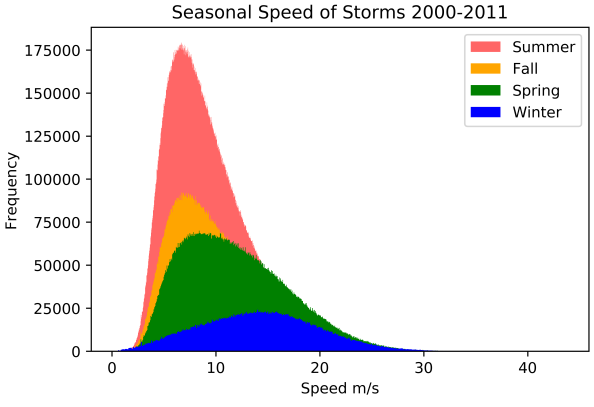

FIG. 10. Histogram showing the average speeds of storms based on season. In confirmation of findings between storm lifetime, and distance traveled, winter has the fastest moving storms.

After observing the seasonal variation between distance traveled and noting the lack of variation in the means of storm lifetime based on season, another question that may arise is how fast these storms are moving. To answer this question the average speed of the storm throughout its whole lifetime was found, and all storms were binned and separated seasonally. In accordance to the furthest moving storms wintertime harbors the fastest moving storms, while summertime the slowest (Fig. 10). The speed distributions have considerably different shapes, and it was decided to look into standard deviations for this question as well. Spring has a standard deviation of 5.1 m/s, summer 3.9 m/s, fall 4.64 m/s and the largest standard deviation was found in the wintertime distribution with 5.6 m/s.

The reason for this seasonal difference in the speed of storms is thought to be tied to wintertime extra-tropical cyclones. It is expected that these larger synoptic events would have a stronger flow. When wintertime storms do materialize, they end up moving much faster under this stronger flow. During the summer, synoptic events are less frequent and mean flow is typically weaker leading to slower moving storms. Another object of interest is the breadth of each of the curves. The largest mean and median values of speed in winter and also see the largest standard deviation of the data compared to fall and summer with much sharper peaks.

TABLE 2. Averages found for extra climatologies of interest.

Season	*Lifetime*	*Distance*	*Expanse*	*Speed*
Winter	2639 s	31.46 km	40.88 km^2	14.17 m/s
Spring	2787 s	30.21 km	58.83 km^2	11.91 m/s
Summer	2790 s	22.43 km	57.80 km^2	9.15 m/s
Fall	2787 s	25.15 km	46.91 km^2	10.31 m/s

TABLE 3. Median values of extra climatologies of interest.

Season	*Lifetime*	*Distance*	*Expanse*	*Speed*
Winter	2100 s	23.21 km	15.99 km^2	14.11 m/s
Spring	2100 s	21.78 km	24.70 km^2	11.25 m/s
Summer	2100 s	16.06 km	27.55 km^2	8.42 m/s
Fall	1801 s	18.14 km	20.86 km^2	9.43 m/s

The final question of interest looked into the velocity dispersions of storms. When comparing the seasonal differences, the magnitude of the eastern and northern velocity changes in accordance to the season. That being said the mean direction of the storm's motion does not change significantly . The found direction of the motion of the storm varies close to none between winter, spring, and summer (Table 4). There is a slight deviation in fall storms but the mean direction is still northeast.

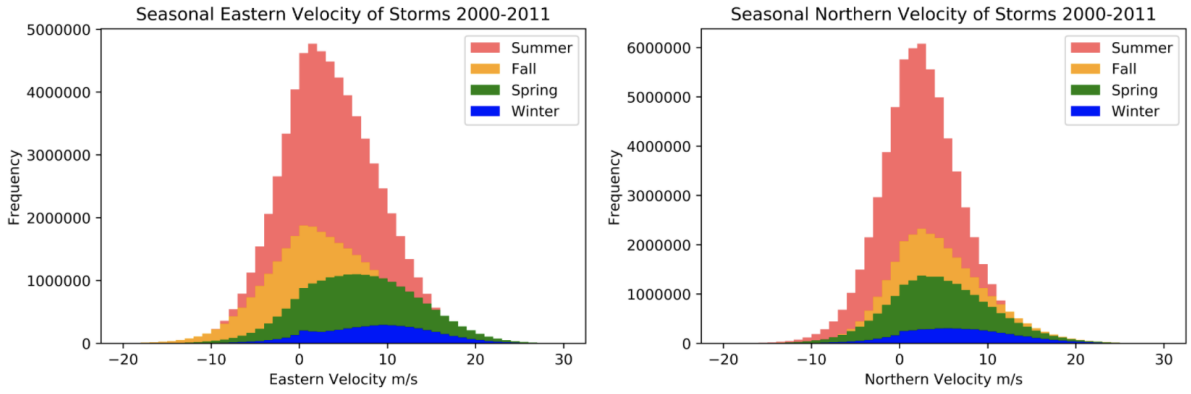

FIG. 11. Histogram showing velocities in both the eastern and northern directions and their respective dispersion.

TABLE 4. Table showing the directions of the storms motion for each season.

Season	*Direction*
Winter	37.97°NE
Spring	34.59°NE
Summer	35.66°NE
Fall	54.52°NE

5. Summary and Conclusions

Due to the absence of research surrounding storm life cycles over the CONUS, a preliminary investigation evaluating both temporal and spatial characteristics of storms is preformed. Data is gathered using the NEXRAD network and compiled into the MYRORSS dataset. MYRORSS data is then run through a redefined version of the storm tracking algorithm developed in Homeyer et al. (2017). Storms tracked are required to be 40-dBZ echo-tops at a minimum height of 4km above sea level with a minimum lifetime of 15 minutes. Data is processed for a period of 12 years starting in January of 2000 and continuing through December 2011. Seasons are defined by 3 month periods where winter included the months of Dec-Feb, spring included Mar-May, summer Jun-Aug, and fall Sep-Nov. Over 12 million 40-dBZ echo-tops are identified using the established criteria placing an average amount of storms per year as just over one million.

a. Temporal Analysis

While investigating the temporal characteristics of storms, it is found that the most storm active season is summer. The second most active season is fall, and this may be due to the high amount of storm activity in September. Winter is the least active of all seasons in storm frequency and this is evident in all the maps shown in the analysis.

Another characteristic observed concerning temporal characteristics is the lifetime of a storm. The average lifetime of a storm in winter is the shortest with a mean of 44 minutes and a median of 30 min, while the longest storms occur in the summer with a mean lifetime of 46.5 min and a median of 35 min. The differences between the medians are skewed because the data in MYRORSS comes in 5-minute increments. This means that a 300 sec difference between any two successive readings is always present and that the median value may not be indicative of a true median lifetime of a 40-dBZ echo-top. Because of this, more accurate statistics are the mean values, which point to a consistent lifetime among all seasons.

b. Spatial Analysis

Spatial mappings comparing storm birth, death, and passage between each season showed somewhat expected results. Over the CONUS, the southeast is by far the most storm active region, and throughout all seasons, Florida appears as the most storm active state. Storm activity trails along the coast of the Gulf of Mexico and is especially prevalent during summer months. Another notable feature is the storm activity created by the Gulf Stream, coming to its maximum off the coast of North Carolina. This feature is observable in all seasons and is the most storm active region on the maps. Western features are highly dependent on geography, this is seen in southern Arizona and New Mexico, but also in southern and Baja California as well as the Rocky Mountains.

An artifact in the spatial maps is the presence of concentric rings and cones of silence over the radars in NEXRAD, which provide the radar data for MYRORSS. This misidentification is likely the result of limited vertical sampling rather than relevant convective cores. The ring patterns are likely due to the different scanning tilts of the radars, and possible mitigation of these artifacts are discussed in future works.

c. Additional Results

When concerning the spatial expanse of storms, it is found that summertime storms are much larger than other seasons. The wings of this exponential decay reach 400 km, where 40-dBZ echo-tops are still being created by the tracking algorithm. The operational definition of storm expanse used is the area of the largest polygon assigned to any storm during its lifetime. This is not the same as finding the spatial expanse of all storms throughout their lifetime, using a different definition will yield different results.

The analysis on the distance traveled by each storm shows that wintertime storms travel the furthest. It should be stressed that the analysis on the distance traveled shows only the distance along a great circle between the first and last position of the storm centroid. For any storm that does not travel along this great circle path, the results from the distance traveled will prove to be an underestimate. These results should be thought of as a lower limit of distance traveled by storms based on the season.

An interesting observation of the seasonal speed distributions is the difference in curve breadth. Differences in the means are thought to be caused by a higher frequency of synoptic scale systems in winter compared to summer. These larger systems are associated with stronger degrees of flow and thus faster moving storms. This does not explain why there would be a different distribution in storm speeds and is an interesting question. Finally, when observing the velocity distributions, the mean directions of motion for storms were almost identical besides the mean direction for fall storms.

d. Future Work

The breadth of this project touched on many different properties of storms over the CONUS and is far from a complete study. Now, possible avenues for future work will be discussed.

One way to shed light on the times of storm activity over the CONUS is for a spatial map showing storm activity based on hours of the day. This map could show how storm activity progresses throughout a diurnal cycle, and would also help differentiate times of storm activity from the East and West Coast.

The presence of local radar returns from low-level signatures appearing in concentric rings on the spatial maps could evaded if the storm tracking algorithm criteria are changed. A trial "Band-Aid" was placed on the tracking algorithm to take storms that lasted only 30 minutes or longer. This cut the dataset significantly and did not prove to be helpful. The hypothesized reason for these signatures is the limited vertical sampling far away from the radar. Nearby, the radar may sample low-level radar signatures because of the better vertical sampling. This means it is more likely to observe low-level precipitation and non-meteorological radar signatures. Because this study looks for signatures of convection, increasing the height threshold of the tracking algorithm would cut out low-level radar signatures, and better identify relative convective cores. Instead of 4 km, bumping the threshold up to 6 km, 7 km, or even 8km would hopefully cut out much of this lower level radar returns from non-convective events.

With regards to the spatial expanse, re-framing how spatial expanse was defined could show how 40-dBZ echo-tops evolve throughout their lifetimes. This would provide information on the scale, and seasonal variation of 40-dBZ echo-tops. The distance traveled statistics would also benefit from a change in operational definition. Currently, distances are found on a path of a great circle cutting through the first and last position of the storm's centroid. If instead, the distance between each successive centroid is found, a more accurate result for distance traveled by each storm would be achieved. Two additional questions surrounding the speeds and velocities associated with the storms would be "Why is there such a change in distributions of the storms' speed?" and "What causes the change in mean direction of the storms during fall?". These two questions would help understand the variation in storms between seasons.

Acknowledgments. The author would like to thank the IDEA Lab group under Dr. McGovern, Melanie Schroers, Jacqueline Waters, Elisa Murillo, Dr. LaDue, and the National Weather Center Research Experience for Undergraduates for their help and ideas that helped make this project come to fruition. The computing for this project was performed at the OU Supercomputing Center for Education and Research (OSCER) at the University of Oklahoma (OU). Also, special thanks are due to mentors involved in the project; Dr. Cameron Homeyer, Ryan Lagerquist, Dr. Amy McGovern, and Thea Sandmæl.

This material is based upon work supported by the National Science Foundation under Grant No. AGS-1560419.

References

Augustine, J. A., and K. W. Howard, 1988: Mesoscale convective complexes over the united states during 1985. *Monthly Weather Review*, **116 (3)**, 685–701, doi: 10.1175/1520-0493(1988)116⟨0685:MCCOTU⟩2.0.CO;2, URL https://doi.org/10.1175/1520-0493(1988)116⟨0685:MCCOTU⟩

2.0.CO;2, https://doi.org/10.1175/1520-0493(1988)116⟨0685:MCCOTU⟩2.0.CO;2.

Homeyer, C. R., J. D. McAuliffe, and K. M. Bedka, 2017: On the development of above-anvil cirrus plumes in extratropical convection. *Journal of the Atmospheric Sciences*, **74 (5)**, 1617–1633, doi:10.1175/JAS-D-16-0269.1, URL https://doi.org/10.1175/JAS-D-16-0269.1, https://doi.org/10.1175/JAS-D-16-0269.1.

Jain, A., 1989: *Fundamentals of Digital Image Processing*. Prentice Hall, 569 pp.

Lakshmanan, V., B. Herzog, and D. Kingfield, 2015: A method for extracting postevent storm tracks. *Journal of Applied Meteorology and Climatology*, **54 (2)**, 451–462, doi:10.1175/JAMC-D-14-0132.1, URL https://doi.org/10.1175/JAMC-D-14-0132.1, https://doi.org/10.1175/JAMC-D-14-0132.1.

Lakshmanan, V., K. Hondl, and R. Rabin, 2009: An efficient, general-purpose technique for identifying storm cells in geospatial images. *Journal of Atmospheric and Oceanic Technology*, **26 (3)**, 523–537, doi:10.1175/2008JTECHA1153.1, URL https://doi.org/10.1175/2008JTECHA1153.1, https://doi.org/10.1175/2008JTECHA1153.1.

Lakshmanan, V., T. Smith, K. Hondl, G. J. Stumpf, and A. Witt, 2006: A real-time, three-dimensional, rapidly updating, heterogeneous radar merger technique for reflectivity, velocity, and derived products. *Weather and Forecasting*, **21 (5)**, 802–823, doi:10.1175/WAF942.1, URL https://doi.org/10.1175/WAF942.1, https://doi.org/10.1175/WAF942.1.

Ortega, K., T. Smith, J. Zhang, C. Langston, Y. Qi, S. Stevens, and J. Tate, 2012: The multi-year reanalysis of remotely sensed storms (myrorss) project, Norman, OK. NOAA/Office of Oceanic and Atmospheric Research under NOAA - University of Oklahoma, https://ams.confex.com/ams/26SLS/webprogram/Paper211413.html.

Starzec, M., C. R. Homeyer, and G. L. Mullendore, 2017: Storm labeling in three dimensions (sl3d): A volumetric radar echo and dual-polarization updraft classification algorithm. *Monthly Weather Review*, **145 (3)**, 1127–1145, doi:10.1175/MWR-D-16-0089.1, URL https://doi.org/10.1175/MWR-D-16-0089.1, https://doi.org/10.1175/MWR-D-16-0089.1.